LONG-TERM TRENDS IN IONOSPHERIC INDICES OF SOLAR ACTIVITY

© 2025 M. G. Deminov

Pushkov Institute of Terrestrial Magnetism, Ionosphere, and Radio Wave Propagation, Russian Academy of Sciences (IZMIRAN), Moscow, Troitsk, Russia

e-mail: deminov@izmiran.ru

Received June 05, 2024

Revised July 18, 2024

Accepted July 25, 2024

Abstract. The results of identifying trends in the annual average ionospheric indices Δ*IG* and Δ*T* are presented, which were obtained after excluding from *IG* and *T* the dependence of these indices on the annual average solar activity indices. The solar activity indices were *F*10, *Ly*-α and *MgII* – solar radiation fluxes at 10.7 cm, in the Lyman-alpha line of hydrogen (121.567 nm) and the ratio of the central part to the flanks in the magnesium emission band 276-284 nm. Two time intervals (in years), 1980–2012 and 2013–2023, are considered. It was found that for the interval 1980–2012 all analyzed linear trends were negative, i.e. Δ*IG* and Δ*T* values decreased over time. They were very weak and insignificant. Fluctuations of Δ*IG* and Δ*T* relative to trends for *Ly*-α were almost twice as large as for *F*10 and *MgII*. In the interval 2013–2023, all analyzed linear trends intensified and became significant, i.e. the rate of decrease in Δ*IG* and Δ*T* over time increased. For *MgII* this rate was almost twice as high as for *F*10. For the interval 2013–2023, the *MgII* index overestimated the contribution of solar radiation to ionospheric indices, especially during the growth phase of solar cycle 25, which began at the end of 2019. As a result, in the growth phase of solar cycle 25, the *F*10 index became a more adequate indicator of solar activity for ionospheric indices than *MgII*. In the interval 1980–2012, the *F*10 and *MgII* indices changed almost synchronously. The growth phase of solar cycle 25 was the first time this synchrony was disrupted for the entire period of *MgII* measurements.

DOI: 10.31857/S00167940250606e1

1. INTRODUCTION

Long-term changes (trends) in the critical frequency of the ionospheric *F2* layer, *foF2*, have been analyzed repeatedly as one of the possible indicators of changes in the middle and upper atmosphere climate (see, for example, recent reviews [Danilov and Konstantinova, 2020; Laštovička, 2022]).

To isolate such changes, much stronger dependencies of *foF2* on extreme ultraviolet (EUV) radiation from the Sun as a source of ionization and heating of the thermosphere must be taken into account. The solar activity indices F10, F30, *Ly*-α and *MgII* are used as an indicator of the Sun's EUV radiation, where *F10*, *F30* and *Ly*-α are the solar radiation fluxes at wavelengths 10.7,30 cm and 121.567 nm, *MgII* is the ratio of central to peripheral emission in the interval 276-284 nm centered at 280 nm [Danilov and Berbeneva, 2023; Laštovička and Burešova, 2023; Laštovička, 2024].

Additional indirect information on *foF2* trends can be obtained from the analysis of ionospheric solar activity indices *IG* and *T.* Indices *T* and *IG* are constructed from experimental data of *foF2* medians of a number of ionospheric stations to replace solar indices in empirical models in order to ensure minimum errors of *foF2* calculation by these models [Liu et al., 1983; Caruana, 1990]. The *IG* or *T* indices are an input parameter to the IRI model [Bilitza, 2018] to replace the *Rz* index in the equation for the median foF2

$$foF2 = a_0 + a_1 Rz, \quad (1)$$

where *Rz* is the international sunspot number (the former version that includes the classical Zurich data series), a_0 and a_1 are coefficients that are determined from the ITU-R maps for a given point, month of the year, and world time [Jones and Gallet, 1962; 1965]. Equation (1) gives the global distribution of *foF2* for a given *Rz*, month of the year, and world time. Substituting *IG* into equation (1) instead of *Rz* usually gives a more accurate global distribution of the median *foF2* for a given month of a given year and world time, since the ionospheric indices are based on *foF2* measurements on that date. Taking into account the dependence of *IG* on the solar activity index, e.g. *F10*, allows us to isolate the *IG* trend, which can serve as an indirect indicator of changes in the upper atmosphere climate.

In the previous work, the trends of the ionospheric indices *IG* and *T* were isolated after excluding their dependences on the solar activity indices *F10* and F30 [Deminov, 2024]. It was obtained, among other things, that the negative trends of the *IG* and *T* indices have intensified in the last decade. The reason for such a property of long-term changes of ionospheric indices remains unknown. It is possible that additional consideration of the solar activity indices *Ly*-α

and *MgII* will allow us to emphasize the features of the ionospheric indices trends in the last decade for different solar activity indices. The solution of this problem was the main goal of this work.

2. SOLAR ACTIVITY INDICES

The initial for the analysis were the monthly averages of the ionospheric and solar activity indices *T*, *IG*, *F10*, *Ly*-α and *MgII*. The *T*, *IG* and *MgII* indices are dimensionless quantities, the *F10* index is measured in 10^{-22} W/(m^{2}Hz), the *Ly*-α index in 10^{15} photon/(m^{2}s). The *T* index is constructed from *foF2* median data at all world time hours for each of the ionospheric stations selected for analysis [Caruana, 1990]. The *IG* index is constructed from the data of *foF2* medians of ionospheric stations at noon [Liu et al., 1983]. The sets of ionospheric stations used to calculate *T* and *IG* are not the same. For this reason, the *T* and *IG* indices may differ for identical conditions, but usually their difference is insignificant.

The *Ly*-α index was derived from Lyman-alpha hydrogen line emission measurements (121.167 nm) on several satellites, which were calibrated against the most reliable of these data. In addition, for periods of no *Ly*-α measurements, the *Ly*-α index was derived from regression equations reflecting the relationship of *Ly*-α to *F10*, *F30*, or *MgII.* Consequently, the *Ly*-α index data for large time intervals are composite (composite) data. Version 4 of such composite *Ly*-α data [Machol et al., 2019] is used below. This version has *Ly*-α index data from 1947 to the present, but *Ly*-α measurements began in mid-1977.Here we use monthly averages of *Ly*-α values in the interval 01.1979-03. 2024, where the month of the year and the year are given. Note that this interval includes the period 04.1989-11.1991, for which missing *Ly*-α data were filled with *MgII* data based on the regression equation of *Ly*-α with *MgII*.

The *MgII* index is also derived from satellite measurements in the band around 276-284 nm as the ratio of the emission intensity at the center of this band (280 nm) to its flanks [Snow et al., 2019]. The *MgII* index data are also composite (composite) data. They start from 01.1979. Here we used monthly averages of *MgII* values in the interval 01.1979-03. 2024.

Using monthly averages of *T*, *IG*, *F10*, *Ly*-α and *MgII* indices, moving annual averages of these indices (T_{12}, IG_{12}, $F10_{12}$, *Ly*-α_{12} and $MgII_{12}$) were obtained for each month of the year in the interval 01.1980-09.2023. The interval 01.1980-12.2010 was chosen as the reference interval for which the correlations between ionospheric and solar activity indices were determined. For this interval, the correlation between the indices T_{12} and IG_{12} is almost complete:

$$T_{12} = 4.0 + 0.947\, IG_{12} \pm 2.1 \qquad (2)$$

With correlation coefficient $K = 0.9993$. The correlation between $Ly\text{-}\alpha_{12}$ and $MgII_{12}$ indices is also quite high:

$$Ly\text{-}\alpha_{12} = -13.4 + 113.7MgII \pm 0.08 \quad (3)$$

with correlation coefficient $K = 0.993$.

To isolate the trends of ionospheric indices IG_{12} and T_{12}, it is necessary to exclude the dependencies of these indices on solar activity, in this case, on indices $MgII_{12}$, $Ly\text{-}\alpha_{12}$ or $F10_{12}$ using regression equations

$$Y_{\text{mod}}(X) = b_0 + b_1X + b_2X^2, \quad (4)$$

where Y is IG_{12} or T_{12}, X is $MgII_{12}$, $Ly\text{-}\alpha_{12}$ or $F10_{12}$. The ionospheric index calculated from equation (4) is a model of this index. It is denoted by $Y_{\text{mod}}(X)$. To determine the coefficients of the regression equations b_j, the data on the analyzed activity indices for 1980-2010 were used. To assess the accuracy of these models, Table 1 shows the correlation coefficients K and standard deviationsσ of measured values of Y from Y_{mod}. The table shows that the accuracies of models (4) are quite high. Nevertheless, the dependences of IG_{12} and T_{12} on $MgII_{12}$ and $F10_{12}$ are more accurate than the dependences of ionospheric indices on $Ly\text{-}\alpha_{12}$. For more clarity, some of these dependences are shown in Fig. 1. From the data in this figure we can see that second degree polynomials are quite accurate approximations of these dependencies.

Table 1.

Fig. 1.

3. LONG-TERM TRENDS OF IONOSPHERIC INDICES

At the previous stage, the models $Y_{\text{mod}}(X)$ were obtained. They are determined by the dependence of the ionospheric index Y_{mod} on the solar index X by regression equation (4). This allows us to find the long-term trends of the indices Y using regression equations, which in linear approximation are of the form:

$$\Delta Y(X) = Y - Y_{\text{mod}}(X) = c_0 + c_1t, \quad (5)$$

where t is the time in years, $c_0$and $c_1$are the coefficients of the regression equation, the values Y and $Y_{\text{mod}}(X)$ are the moving averages for a year of the ionospheric index values from the measurement data and from the model, which are centered at a given month of the year. Ionospheric indices are dimensionless quantities. Therefore, the coefficient $c_1$has the dimension of 1/year. It gives the rate of change of the ionospheric index Y with time, from which the strong dependence of Y on solar activity is excluded using the regression equation $Y_{\text{mod}}(X)$.

One of the objectives of this work was to evaluate the features of ionospheric index trends in the last decade. Therefore, the trends of ionospheric indices were evaluated for the intervals 1980-2012 and 2013-2023.

Table 2.

Table 2 shows the parameters of regression equations (5) for these intervals. It follows from the data in Table 2 that all analyzed trends are negative ($c_1 < 0$). For the interval 1980-2012, they are not significant (correlation coefficients K vary between 0.01-0.23) with strong fluctuations $\Delta Y(Ly\text{-}\alpha_{12})$ relative to the trends ($\sigma = 6.5 \pm 0.1$). For the 2013-2023 interval, all analyzed trends are significant, i.e., they are negative and increase in strength when moving from the 1980-2012 interval to the 2013-2023 interval. The strongest ($c_1 = -2.78$) and weakest ($c_1 = -1.42$) of these trends in the 2013-2023 interval are observed for $\Delta IG_{12}(MgII_{12})$ and $\Delta T_{12}(F10_{12})$. The trends of $\Delta IG_{12}(X)$ and $\Delta T_{12}(X)$ for the coincident X indices differ little, however, the negative trends of $\Delta IG_{12}(X)$ are slightly stronger than the trends of $\Delta T_{12}(X)$.

Fig. 2.

The nature of changes in $\Delta Y(X)$ with time can be seen more clearly from the data in Fig. 2 and Fig. 3. It can be seen from the data in these figures that the scatter of the data with respect to linear trends is indeed large. This scatter is particularly large for $\Delta Y(Ly\text{-}\alpha_{12})$, including the 1989-1991 interval when direct Ly-α measurements were not available and were filled in with $MgII$ data based on a regression equation between Ly-α and $MgII$ [Machol et al., 2019]. The relatively large values of standard deviations σ for $\Delta Y(Ly\text{-}\alpha_{12})$ in the 1980-2012 interval are related to the same reason (see Table 2). Note that Figures 2 and 3 do not show particularly large fluctuations $\Delta Y(MgII_{12})$ for the 1989-1991 interval, in which $MgII$ was used to fill in the missing Ly-α data.

Fig. 3.

Very strong negative trends of $\Delta Y(MgII_{12})$ in the interval 2013-2023 correspond to certain phases of solar cycles. Additional information on the peculiarities of the changes in the trends with solar activity cycles can be obtained by comparing the changes with time of the ionospheric indices Y and the models of these indices $Y_{mod}(X)$. Fig. 4 shows an example of such a comparison for the IG_{12}, $IG_{mod}(F10_{12})$ and $IG_{mod}(MgII_{12})$ indices. This figure shows that the interval 2013-2023 corresponds to the maximum and decline phase of solar cycle 24 and the growth phase of solar cycle 25. It is believed that cycle 25 began at the end of 2019. [Upton and Hathaway, 2023]. From the data in this figure, it can be seen that the strongest deviations of $IG_{mod}(MgII_{12})$ from IG_{12} occurred during the growth phase of solar cycle 25, which led to a strong negative trend $\Delta IG_{12}(MgII_{12}) = IG_{12} - IG_{mod}(MgII_{12})$. For this period, the deviations of $IG_{mod}(F10_{12})$ from

IG_{12} were relatively weak. Hence, the *F10* index is a more accurate indicator of solar activity than *MgII* for the ionospheric *IG* index during the growth phase of solar cycle 25. This statement is also true for the ionospheric *T* index. Additional analysis showed that in the interval 1980-2013 $IG_{mod}(MgII_{12})$ and $IG_{mod}(F10_{12})$ values changed almost synchronously and slightly differed from IG_{12}, i.e., the above-mentioned feature of the *MgII* index at the growth phase of solar cycle 25 was not observed for the entire previous period of measurements of this index.

Fig. 4.

4. CONCLUSION

The ionospheric indices *T* and *IG* were obtained from the medians of *foF2* of a number of ionospheric stations of the Northern and Southern Hemispheres. Therefore, they can serve as indirect indicators of mean changes of *foF2*, including long-term changes of this value. The accuracy of determining *T* and *IG* from *foF2* data is decreased at low solar activity. This follows from equation (1): *foF2* is almost independent of solar activity when the condition $a_0 > a_1 Rz$ is satisfied. Therefore, for example, the deviations of IG_{12} from $IG_{mod}(MgII_{12})$ in Fig. 4 at low solar activity (2019-2020) may be at least partly due to the inaccuracy of the determination of the ionospheric *IG* index. For the growth phase of solar cycle 25 (after 2020), ionospheric index calculations from *foF2* data are more reliable. This suggests that for the solar cycle 25 growth phase the *MgII* index overestimates the contribution of solar activity to the ionospheric *IG* index and, apparently, to *foF2*. In this case, the *IG* index allowed us to identify the interval for which the *MgII* index ceases to be an adequate indicator of solar activity for *foF2*. This statement requires independent verification since *IG* is a proxy index for *foF2*.

The aim of this work was to clarify the features of the trends of the ionospheric indices *T* and *IG* in the last decade by taking into account the additional solar activity indices *MgII* and *Ly*-α . The result was unexpected: for the interval 2013-2023, taking into account *MgII* or *Ly*-α led to even stronger negative trends of ionospheric indices than the generally accepted *F10* index. Therefore, the question about the reason of strengthening in the last decade of negative trends of ionospheric indices and, especially foF2, remains open. It is possible that consideration of monthly averages of the ionospheric and solar indices will allow us to solve this problem to some extent. This requires special consideration, which is beyond the scope of this paper.

5. CONCLUSIONS

The paper presents the results of trend extraction of the year-average ionospheric indices Δ*IG* and Δ*T*, which were obtained after excluding from *IG* and *T* the dependence of these indices on the year-average solar activity indices. The solar activity indices were *F10*, *Ly*-α and *MgII* -

the solar radiation fluxes at 10.7 cm, in the Lyman-alpha hydrogen line (121.567 nm) and the ratio of the central part to the flanks in the magnesium emission band at 276-284 nm. Two time intervals (in years) 1980-2012 and 2013-2023 have been considered. The following conclusions are obtained.

1. For the interval 1980-2012, all analyzed linear trends are negative, i.e., the values of ΔIG and ΔT decreased with time. They were very weak and insignificant. The fluctuations of ΔIG and ΔT relative to the trends for *Ly*-α were almost twice as large as for *F10* and *MgII*.

2. For the 2013-2023 interval, all analyzed linear trends intensified and became significant, i.e., the rate of decrease of ΔIG and ΔT with time increased. For *MgII*, this rate was almost twice as large as for *F10*.

3. For the 2013-2023 interval, the *MgII* index overestimated the solar radiation contribution to the ionospheric indices, especially during the growth phase of solar cycle 25, which started at the end of 2019.This led to high values of the negative trends of the ionospheric indices for *MgII* in this time interval. For *F10*, such a trend was much smaller. As a result, during the growth phase of solar cycle 25, the *F10* index became a more adequate indicator of solar activity for ionospheric indices than *MgII*.

4. In the interval 1980-2012, the *F10* and *MgII* indices changed almost synchronously. The growth phase of solar cycle 25 was the first case of violation of this synchrony in the entire period of *MgII* measurement.

ACKNOWLEDGEMENTS

Solar activity index data were taken from http://www.ukssdc.ac.uk/wdcc1 (WDC for Solar-Terrestrial Physics, UK), ftp.seismo.nrcan.gc.ca/spaceweather (Space Weather Canada), www.sws.bom.gov.au/HF_Systems (Space Weather Services, Australia), https://lasp.colorado.edu/lisird (LASP Interactive Solar Irradiance Datacenter, USA) on 10.04.2024.

FUNDING

The research was supported by the Program of Fundamental Scientific Research in the Russian Federation on the topic: "Study of Solar Activity and Physical Processes in the Sun-Earth System" (No. 1021100714181-3).

CONFLICT OF INTERESTS

The author declares no conflict of interest.

REFERENCES

1. *Danilov A.D., Konstantinova A.V.* Long-term variations in the parameters of the middle and upper atmosphere and ionosphere (review) // Geomagnetism and Aeronomy. V. 60. No. 4. P. 411–435. 2020. https://doi.org/10.31857/S0016794020040045

2. *Bilitza D*. IRI the international standard for the ionosphere // Adv. Radio Sci. V. 16. P. 1–11. 2018. https://doi.org/10.5194/ars-16-1-2018

3. *Caruana J.* The IPS monthly T index / Proc. Solar-Terrestrial Prediction Workshop. Leura, Australia. October 16–20, 1989. V. 2. Ed. R.J. Thompson. Boulder, CO: Environmental Research Lab. P. 257–263. 1990.

4. *Danilov A.D., Berbeneva N.A.* Statistical analysis of the critical frequency *foF*2 dependence on various solar activity indices // Adv. Space Res. V. 72. N 6. P. 2351–2361. 2023. https://doi.org/10.1016/j.asr.2023.05.012

5. *Deminov M.G.* Trends in ionospheric indices of solar activity // Geomagn. Aeron. (Engl. Transl.) V. 64. N 5. 2024.

6. *Jones W.B., Gallet R.M.* The representation of diurnal and geographic variations of ionospheric data by numerical methods // Telecommun. J. V. 29. N 5. P. 129–149. 1962.

7. *Jones W.B., Gallet R.M.* The representation of diurnal and geographic variations of ionospheric data by numerical methods. 2 // Telecommun. J. V. 32. N 1. P. 18–28. 1965.

8. *Laštovička J*. Long-term changes in ionospheric climate in terms of *foF*2 // Atmosphere. V. 13. N 1. ID 110. 2022. https://doi.org/10.3390/atmos13010110

9. *Laštovička J., Burešova D*. Relationships between *foF*2 and various solar activity proxies // Space Weather. V. 21. N 4. ID e2022SW003359. 2023. https://doi.org/10.1029/2022SW003359

10. *Laštovička J.* Dependence of long-term trends in *foF*2 at middle latitudes on different solar activity proxies // Adv. Space Res. V. 73. N 1. P. 685–689. 2024. https://doi.org/10.1016/j.asr.2023.09.047

11. *Liu R., Smith P., King J*. A new solar index which leads to improved *foF*2 predictions using the CCIR atlas // Telecommun. J. V. 50. N 8. P. 408–414. 1983.

12. *Machol J., Snow M., Woodraska D., Woods T., Viereck R., Coddington O*. An improved Lyman-alpha composite // Earth and Space Science. V. 6. N 12. P. 2263–2272. 2019. https://doi.org/10.1029/2019EA000648

13. *Snow M., Machol J., Viereck R., Woods T., Weber M., Woodraska D., Elliott J.* A revised Magnesium II core-to-wing ratio from SORCE SOLSTICE // Earth and Space Science. V. 6. N 11. P. 2106–2114. 2019. https:// doi.org/10.1029/2019EA000652

14. *Upton L.A., Hathaway D.H.* Solar cycle precursors and the outlook for cycle 25 // J. Geophys. Res. – Space. V. 128. N 10. ID e2023JA031681. 2023. https://doi.org/10.1029/2023JA031681

Table 1. Standard deviationsσ and correlation coefficients *K* of regression equations (4) on the data on ionospheric indices of solar activity and solar indices of this activity for 1980-2010.

Y \ *X*	$MgII_{12}$		$Ly\text{-}\alpha_{12}$		$F10_{12}$	
	σ	*K*	σ	*K*	σ	*K*
IG_{12}	4.3	0.997	6.9	0.993	4.5	0.997
T_{12}	3.5	0.998	6.9	0.992	3.6	0.998

Table 2. Correlation coefficients *K*, standard deviations σ and coefficients c_1 (in 1/year) of regression equations (5) from measurements of ionospheric (IG_{12}, T_{12}) and solar ($MgII_{12}$, $Ly\text{-}\alpha_{12}$, $F10_{12}$) indices for 1980-2012 and 2013-2023.

ΔY\X	$MgII_{12}$			$Ly\text{-}\alpha_{12}$			$F10_{12}$		
	c_1	σ	*K*	c_1	σ	*K*	c_1	σ	*K*
	1980-2012								
IG_{12}	-0.06	4.3	0.14	-0.14	6.6	0.20	-0.11	4.3	0.23
T_{12}	-0.004	3.5	0.01	-0.08	6.4	0.13	-0.004	3.5	0.12
	2013-2023								
IG_{12}	-2.78	4.8	0.88	-2.71	4.6	0.92	-1.45	3.0	0.83
T_{12}	-2.74	3.1	0.94	-2.66	2.1	0.97	-1.42	3.7	0.77

Figure captions

Fig. 1. Dependences of ionospheric indices T_{12} and IG_{12} on solar activity indices $MgII_{12}$ and $Ly\text{-}\alpha_{12}$ according to the measurement data and regression equations (4) - points and solid lines; K andσ - correlation coefficients and standard deviations of these equations.

Fig. 2. Changes in the index $\Delta IG_{12}(X)$ with time in years from experimental data (dots) and linear interpolations (trends) of these data - solid lines.

Fig. 3. Changes in the $\Delta T_{12}(X)$ index with time in years from experimental data (dots) and linear interpolations (trends) of these data are solid lines.

Fig. 4. Changes with time in years in the IG_{12} index (thick line) and models of this index $IG_{mod}(F10_{12})$ - thin line and $IG_{mod}(MgII_{12})$ - dashed line.

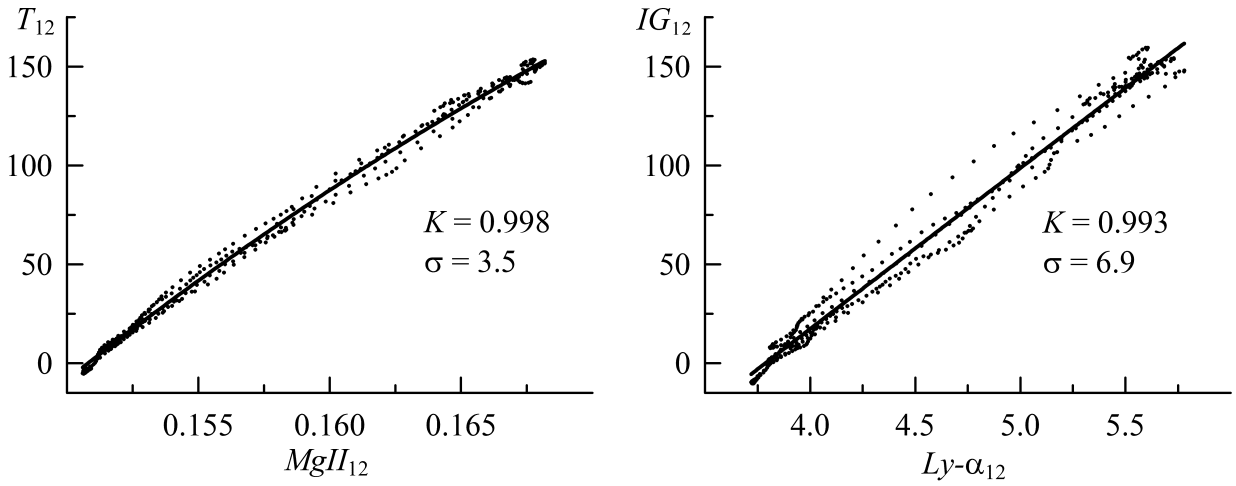
T_{12}
150
100
50
0
0.155
0.160
0.165
$MgII_{12}$
$K = 0.998$
$\sigma = 3.5$
IG_{12}
150
100
50
0
4.0
4.5
5.0
5.5
$Ly\text{-}\alpha_{12}$
$K = 0.993$
$\sigma = 6.9$

Fig. 1.

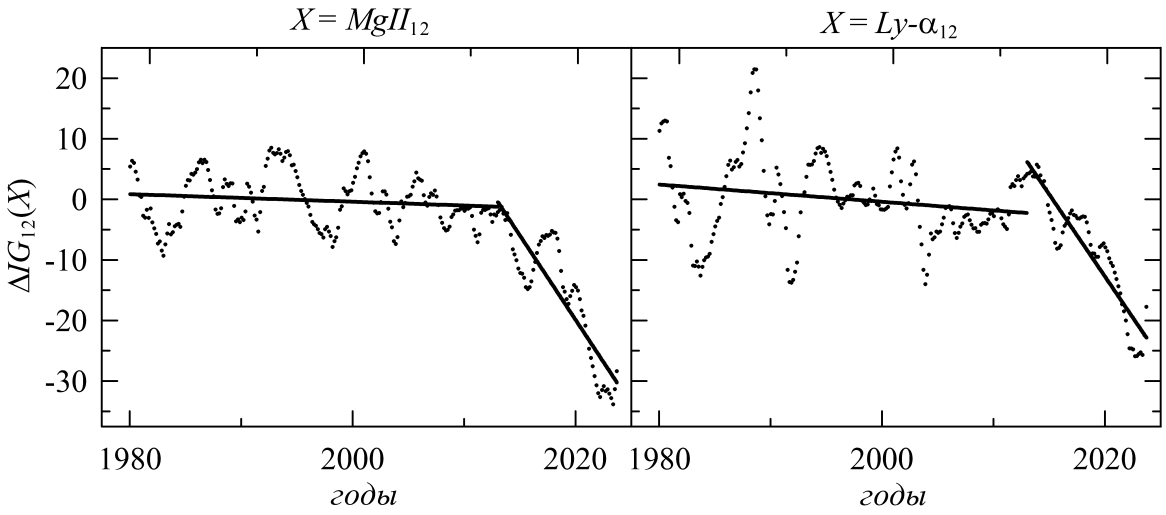
X = MgII12
X = Ly-α12
20
10
0
-10
-20
-30
ΔIG12(X)
1980
2000
2020
годы
1980
2000
2020
годы

Fig. 2.

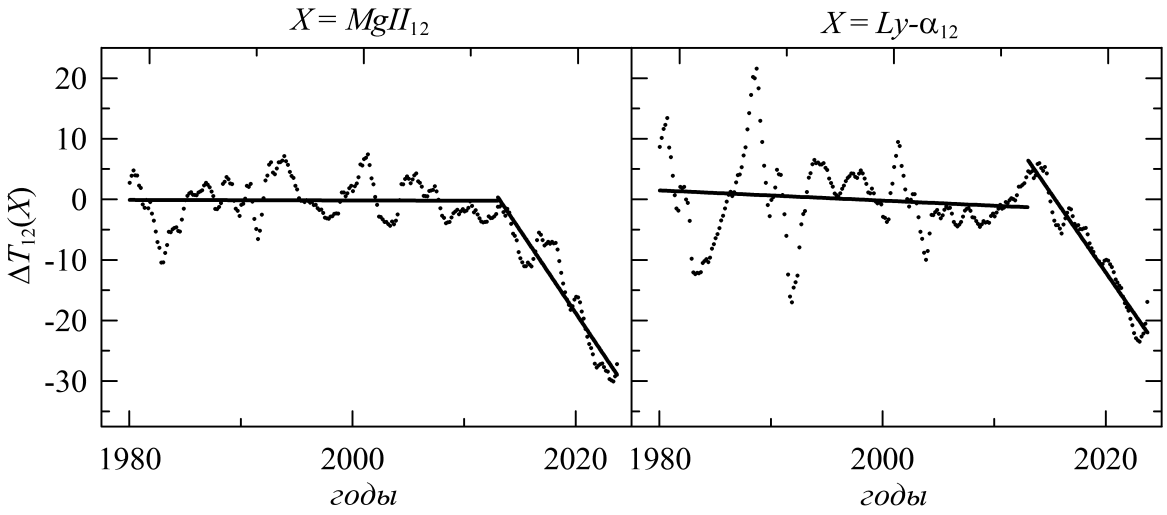

Fig. 3.

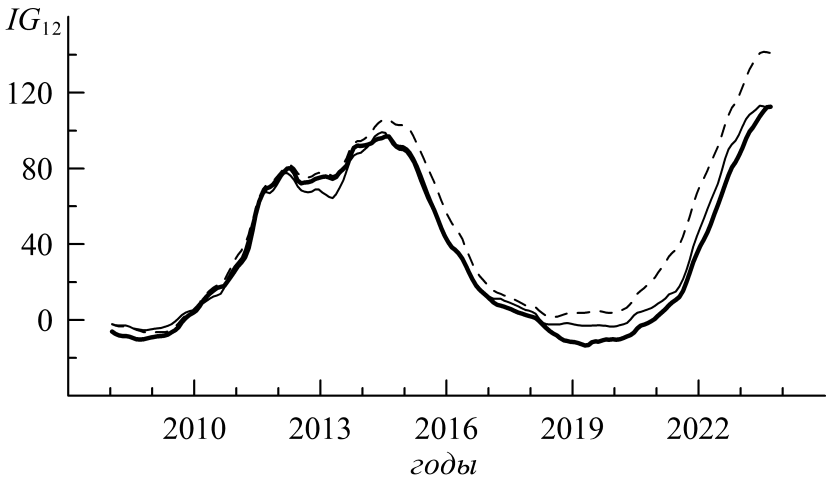

Fig. 4.